Predictions of ENSO with a Coupled Atmosphere–Ocean General Circulation Model①

Zhou Guangqing (周广庆) and Zeng Qingcun (曾庆存)

LASG, Institute of Atmospheric Physics, Chinese Academy of Sciences, Beijing 100029

(Received September 18, 2000; revised March 7, 2001)

P42 A

ABSTRACT

Predictions of ENSO are described by using a coupled atmosphere–ocean general circulation model. The initial conditions are created by forcing the coupled system using SST anomalies in the tropical Pacific at the background of the coupled model climatology. A series of 24–month hindcasts for the period from November 1981 to December 1997 are carried out to validate the performance of the coupled system. Correlations of SST anomalies in the Nino3 region exceed 0.54 up to 15 months in advance and the rms errors are less than 0.9°C. The system is more skillful in predicting SST anomalies in the 1980s and less in the 1990s. The model skills are also seasonal–dependent, which are lower for the predictions starting from late autumn to winter and higher for those from spring to autumn in a year–time forecast length. The prediction, beginning from March, persists 8 months long with the correlation skill exceeding 0.6, which is important in predictions of summer rainfall in China. The predictions are succesful in many aspects for the 1997–2000 ENSO events.

Key words: CGCM, Initialization, ENSO prediction

1. Introduction

El Niño and Southern Oscillation (ENSO) is the most prominent phenomenon of interannual climate variability in the tropical Pacific ocean–atmosphere system, and prediction of ENSO variability is potentially important because its impact is significant on the global short–term climate anomalies. The tropical Pacific sea surface temperature (SST) anomaly is one of the crucial factors that affect the summer monsoon precipitation in China (Huang and Wu., 1989; Wang, 1997), especially in the southeast of China where the economy is most developed and the population is most inhabited. The predictions of ENSO play an important role in the summer rainfall forecast in China (Wang, 2000; Lin et al., 1999, 2000).

The dynamics and predictability of ENSO have been major topics in many wordwide research projects since the 1980s (e.g. CLIVAR). Simulated by pioneering work of Cane et al. (1986), a number of forecast systems with varying complexity have been developed and tested for predicting ENSO variability (Latif et al., 1998). Hindcast experiments with the different systems have shown that the models have the potential to make useful forecasts for seasonal to interannual time scales (Cane et al., 1986; Latif et al., 1993; Ji et al., 1996, 1997; Kirtman et al., 1997; Latif et al., 1998). In forecast mode, however, the predictive skills highly depend on

①This Project is Supported by Key Program of Chinese Academy of Sciences KZCX2–203, National Key Program for Developing Basic Sciences G1999032801, and National Natural Science Foundation of China (Grant No. 49735160 and 40005007)

the model's configuration and the forecast cases. Therefore, It is necessary to improve ENSO predictions by developing different types of forecast systems with their own unique features. In principle, a coupled atmosphere–ocean general circulation model (CGCM) is most powerful way to produce the best forecast because of its faithful approximation to the dynamics of ENSO. However, the problems of climate drift and initial shock prevent the coupled GCMs from achieving their potential (Schneider et al., 1999).

Some progress has been made in seasonal to interannual climate prediction in China, especially, based on a coupled atmosphere–ocean GCM, a semi–operational short–term climate prediction system has been established in Institute of Atmospheric Physics (IAP), Chinese Academy of Sciences (CAS) (Zeng et al., 1997). In 1999, a coupled atmosphere–ocean general circulation model for the tropical Pacific (IAP TP–CGCM) was developed in which the oceanic component was a free surface model with higher resolution and the statistic technique was applied to remove the 'climate drift' in the coupling scheme (Zhou et al., 1999). A long time free integration was carried out to validate the coupled model's performance, indicating that the ENSO–like interannual variability was re–produced quite well.

In this paper, an ENSO prediction system is developed based on IAP TP–GCM. Through designing an anomalous initialization scheme in which the balance between the component models in initial conditions is taken into account, a series of SST anomaly hindcasts in the tropical Pacific up to 24 months lead time have been carried out, one hincast per month for the period from 1982 to 1997. In Section 2, the model's configuration and performance are described; the anomalous initialization is designed in Section 3; the hindcast experiments and some near real–time predictions for 1997 / 1998's El Niño and 1999 / 2000's La Niña are presented in Sections 4 and 5, respectively; and a summary is given in Section 6.

2. Coupled model and its simulation

A coupled atmosphere–ocean–land model with some unique characteristics was designed by Zeng (1983) (referred as IAP–type models), e.g. calculation of the departures of thermodynamic variables in time integration by subtracting the standard stratification, a unified vertical coordinate (σ–coordinate) for both atmosphere and ocean, total available energy consideration of the coupled system for not only the differential but also finite–difference system, free surface treatment for the oceanic GCM, consistent treatment for the boundary terms and boundary conditions at the interface of atmosphere–ocean and atmosphere –land, and so on. The coupled model used in this paper combines the IAP 2–L global atmosphere GCM (AGCM) and the IAP tropical Pacific oceanic GCM (OGCM) with free surface. Brief descriptions of the component models, the coupling procedure and the coupled simulation are given below.

2.1 *Atmospheric model*

The atmosphere model is a global grid point model that was designed and developed at IAP (Zeng, 1983; Liang, 1986, Zeng et al., 1989). The horizontal resolution of the atmospheric model is 4° in latitude and 5° in longitude. The vertical structure is represented by two equal mass layers that is formulated in σ–coordinate between the surface and 200 hPa. The model fully adopts standard physics such as longwave radiation, cloud–radiation feedback, convective processes, boundary layer treatment, ground surface hydrology and so on developed by Oregon State University (OSU) (Ghan et al, 1982) with appropriate modification and

improvements (Liang, 1986). The boundary layer, although it is not explicitly treated, is parameterized as a constant flux surface layer of undefined thickness.

The atmosphere GCM has been used in a variety of climate simulation and sensitivity experiments. These results show that this AGCM is able to reproduce the observed climatology and variations of global atmosphere when forced by prescribed boundary conditions (Liang, 1986; Zeng et al., 1997; Zeng et al., 1990).

2.2 *Ocean model*

The ocean model is a free surface tropical Pacific Ocean general circulation model described by Zhang and Endoh (1992). The domain extends from 121°E to 69°W between 30°S and 30°N in the tropical Pacific Ocean, and has realistic coastline in the east and west boundaries. The model's horizontal grid lengths are 1° in latitude and 2° in longitude, and in the vertical, there are 14 layers with 20 m resolution in the upper 60 m and 30 m resolution between 60m and 240 m depth. The flat-bottom is 4000 m deep. In time integration the barotropic and baroclinic modes are calculated separately with the time step taken as 5 minuts for the barotropic mode and 2 hours for the baroclinic mode, respectively. The horizontal eddy viscosity is 2×10^3 m^3 s^{-1} equatorward of 10° latitude; poleward of this, it increases linearly to 3×10^4 m^3 s^{-1} at 30°N (S); the lateral eddy diffusivity for temperature and salinity is held constant at a value of 2×10^3 m^3 s^{-1}; the vertical eddy viscosity and diffusivity are dependent on the Richardson number (Pacanowski and Philander, 1981). The lateral boundary conditions are non-slip and non-flux conditions; however, along the model northern and southern boundary, the temperature and salinity equations gain an additional Newtonian term for their relaxation to the observations (Levitus, 1982).

The model has been tested in several numerical simulations and the results show that the OGCM has reproduced realistic climatology and interannual variability, respectively, when forced by observed fluxes (Zhang and Endoh, 1992, 1994).

2.3 *Coupling*

The coupled GCMs, in general, suffer the difficulty of the so-called "climate drift" which shows the model's severe discrepancies in climatology from the reality. The realistic climatology is the foundation for simulating and predicting climate variations. Therefore, some methods, e.g. flux correction or anomaly coupling, are used to reduce the climate drift and cause the coupled model's climatology of the target fields (such as SST, wind stress, sea level pressure, and so on) to be close to the observations.

In this present work, the so-called 'statistical correction' method (SCM) is developed to modify the atmospheric variables at the models' air-sea interface (Zhou et al., 1999). Because only the winds at approximately 400 hPa (V_{400}) and 800 hPa (V_{800}) can be predicted by AGCM, the surface wind (V_S) is extrapolated externally from those of the tow model levels by

$$V_S = 0.7(1.5V_{800} - 0.5V_{400}) . \tag{1}$$

Numerical analyses have shown that there are systematic errors in such externally extrapolated surface winds compared with the corresponding observations. In order to reduce these systematic errors, a statistical relation between the surface winds and those at the model levels is constructed as

$$V_S = a_0 + a_1V_{800} + a_2V_{400} , \tag{2}$$

where a_0, a_1, and a_2 are space-dependent coefficients determined by statistical regression. The numerical experiment shows that this is a method effective in reducing the systematic errors of AGCM in the uncoupled mode. The above correction is carried out by means of making the annual mean errors minimum and the phases of annual cycle are maintained by the model.

In uncoupled mode of OGCM, the heat flux formulation is usually calculated as a relaxation of the simulated SST to the observed climatology (Haney, 1971). In coupled mode, however, considering the realistic heat flux feedback between the ocean and atmosphere, the following formula is used:

$$Q_T = S - R - LE_s - H \tag{3}$$

where Q_T and S are the net heat flux and net solar radiation absorbed by ocean, respectively, R,LE_S and H are the net upward long-wave radiation, latent heat flux and sensible heat flux at the sea surface, respectively, and

$$R = Q^* \cdot \sigma T_g^4 , \tag{4}$$

$$Q^* = 0.985 \times (0.39 - 0.05\sqrt{e_A})(1 - 0.6 \times n_c^2) , \tag{5}$$

$$LE_S = \rho_A C_D V_A L \cdot [q_S(T_g) - q_A] , \tag{6}$$

$$H = \rho_A C_D V_A C_p \cdot [T_g - T_A] , \tag{7}$$

where T_g and T_A are the sea surface temperature and the air temperature, respectively, e_A, the air vapour pressure, n_c, the fraction of cloud cover, ρ_A and V_A, the atmospheric density and the wind speed at sea surface, respectively, q_A and q_S, the specific humidity and saturate specific humidity at T_g, respectively, σ, the Stefan-Boltzmann constant. Furthermore, the SCM is used to modify the above variables.

The SST predicted by OGCM acts directly as the forcing of the atmospheric model without any modification. Outside the OGCM's domain, the climatological SST with annual cycle is adopted. The fluxes between the two component models are exchanged once a day, i.e. the synchronously coupling.

2.4 *Coupled model simulation*

A 100-year integration of the coupled model was carried out. The initial conditions were taken respectively from the 10-year-long simulations of the two component models with observed forcing. The last 40-year coupled integration were used to define the coupled model climatology.

The annual-mean SST field in the tropical Pacific simulated by the coupled model is shown in Fig. 1a, in which many characteristics agree very well with the corresponding observations (Fig. 1b), e.g. the tongue of cold water in the eastern equatorial Pacific which extends westward along the equator from the South American coast and the warm pool in the western Pacific. Figure 2 shows the vertical section of the sea temperature along the equator. The thermocline, which is distinguished by great temperature gradient in the vertical, was simulated quite well (Zhou et al., 1999). The main features of seasonal variation were also simulated which present as spring warming and fall cooling in the eastern equatorial Pacific. But the westward propagation of seasonal transition was not simulated well.

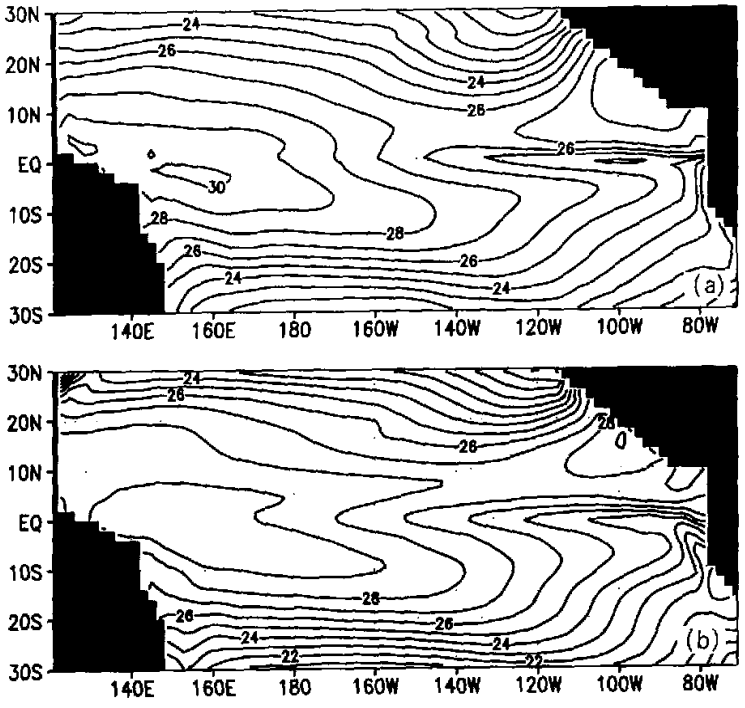

Fig. 1. Simulated (a) and observed (b) annual mean SST. Contour interval is 1°C.

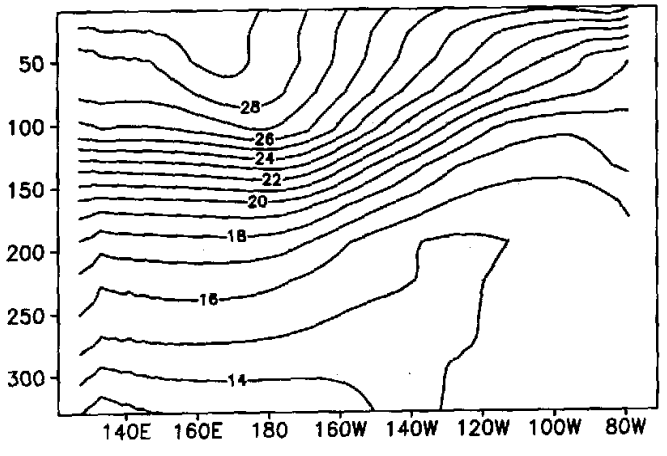

Fig. 2. Longitude–depth section of simulated annual mean sea temperature along the equator. Contour interval is 1°C.

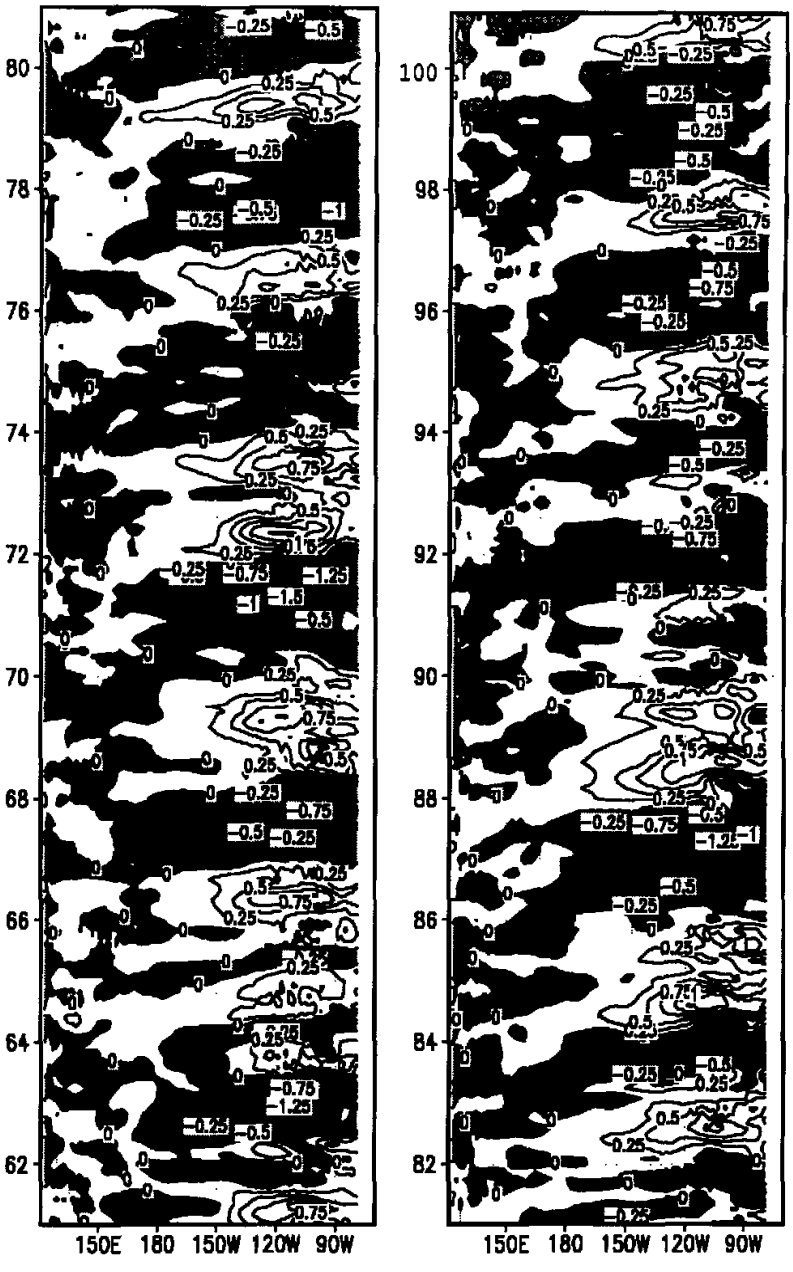

Fig. 3. Longitude–time section of simulated sea surface temperature anomalies along the equator. Contour interval is 0.25°C.

Realistic interannual variability is also important to the coupled model tests. Figure 3 shows the equatorial Pacific SST anomalies. Peaks of warm and cold events are generally in the far eastern Pacific with the amplitudes of about 1.5°C, weaker than the obvserved. The SST anomalies vary on interannual time scales similar to ENSO cycle and show a little phase propagation. Further analysis shows that the anomalies of heat content in the upper ocean, which is defined as vertical–averaged temperature, propagate eastward along the equator and westward off the equator, consistent with the delayed oscillator mechanism (Suarez and Schopf, 1988; Battisti and Hirst, 1989).

3. Initial condition

There is an evidence that coupled predictions depend sensitively on initial conditions (Ji and Leetmaa, 1997). If this is the case, the realistic initial states from which the coupled predictions begin are crucial. On the other hand, however, there are still deficiencies in the model's simulation even though the climate drift has been reduced and the imbalance between the model and initial conditions generally exists if it is not modified properly. Therefore, model's adjustment to these unbalanced initial conditions will occur and the expected predictions will be disturbed when predictions begin from these initial conditions. This adjustment procedure is referred as initial shock.

At the present work, an initialization scheme for the coupled system is developed to avoid the problem of initial shock. In the hypothesis that the memory of ENSO variability are contained in ocean and keeping in mind that the balance between the coupled system and initial states is important for good predictions (Schneider et al., 1999), only the observed sea surface temperature anomaly in the tropical Pacific is used to initialize the model. The procedure is that from the states of the coupled model at year 100, the initial conditions for the atmosphere are first created by forcing AGCM with the observed SST anomalies added to the coupled model's climatology; at the same time of AGCM integration, the output of the AGCM, including the wind stress and heat flux, is used to force OGCM to create oceanic initial conditions.

In fact, the above procedure is performed in quasi–coupled mode. The initial conditions are created through inducing the actual interannual phases by using observed SST anomalies

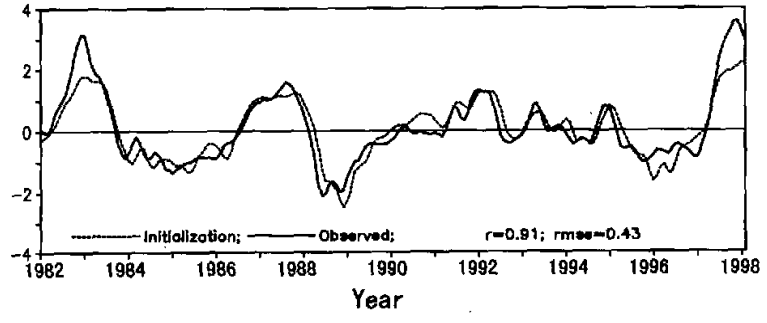

Fig. 4. Time curves of SST anomalies in Nino3 region (150°–90°W, 5°S–5°N). Solid line: observation; dashed line: initializing results.

at the background of the coupled model climatology. Therefore, the balances between the models and initial conditions and between atmosphere and ocean in initial states are achieved. The initializing procedure is continuously carried out for the period of November 1981 to December 1997 using the analyzed data of Reynolds (1994). The results show that the simulated SST anomalies in Nino3 (150°–90°W, 30°S–30°N) are close to the observation with correlation of 0.91 (Fig. 4).

4. Hindcast experiments

194 hincast experiments, starting from the end of every month for the period of November

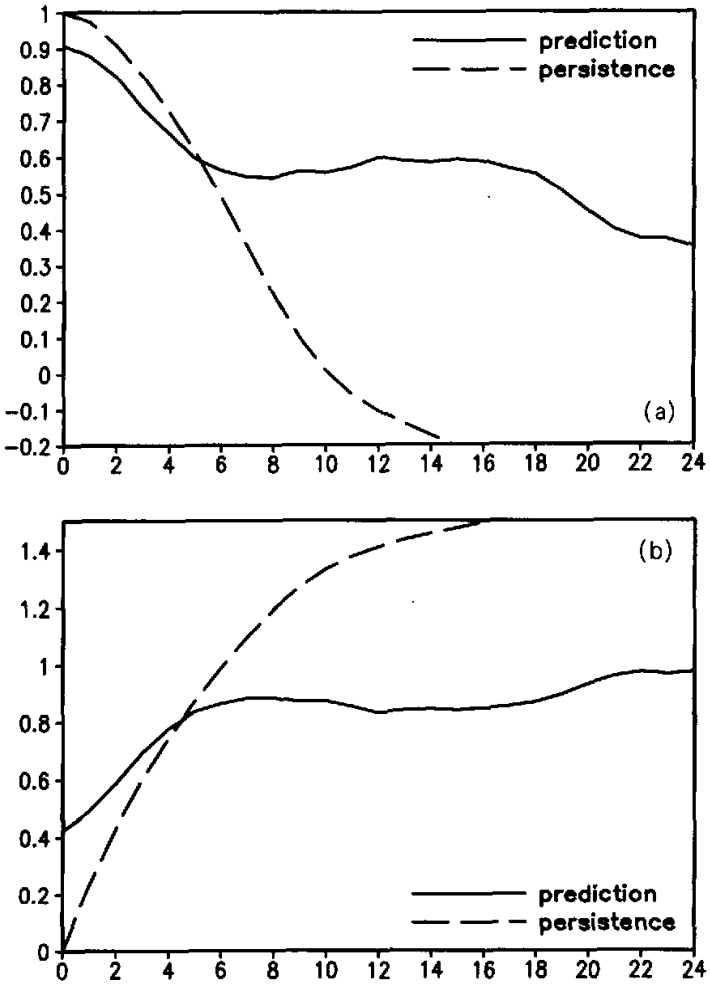

Fig. 5. Correlations (a) and root–mean–square errors (b) with observation for forecast (solid line) and persistence (dashed line), respectively.

1981 to December 1997, were performed. Each hincast had been integrated for 24 months, and a set of forecast climatologies was defined as the mean of the hindcasts with the same lead time. In this section, we discuss the skill of hindcast anomalies from this set of climatologies respectively.

3.1 *General statistics*

The anomaly correlations and root mean square (rms) errors of the predicted SST anomalies averaged over Nino3 region are shown in Fig. 5. Also shown are the ones by persisting the observed SST anomalies from the same initial times as a reference. Although the forecast skills decrease with lead time, the forecasts are skillful at least up to more than 15 months in advance with the correlations above 0.54, in particular for the predictions exceeding 4 months in advance which show much higher skills than persistence. During initial 4 months, the forecast skills are lower than the persistent ones. This is mainly attributed to less thermocline accuracy of ocean in initial conditions. In facts, most dynamical forecast systems without subsurface oceanic data assimilation perform in similar ways. Therefore, it is important to insert oceanic subsurface data in the forecast system for improving prediction skill. The rms errors have a coherent relation with correlation skills, which grow with forecast length. The mean rms errors are less than 0.89°C at lead time of 15 months and much smaller than persistent ones after 4 months from initial time.

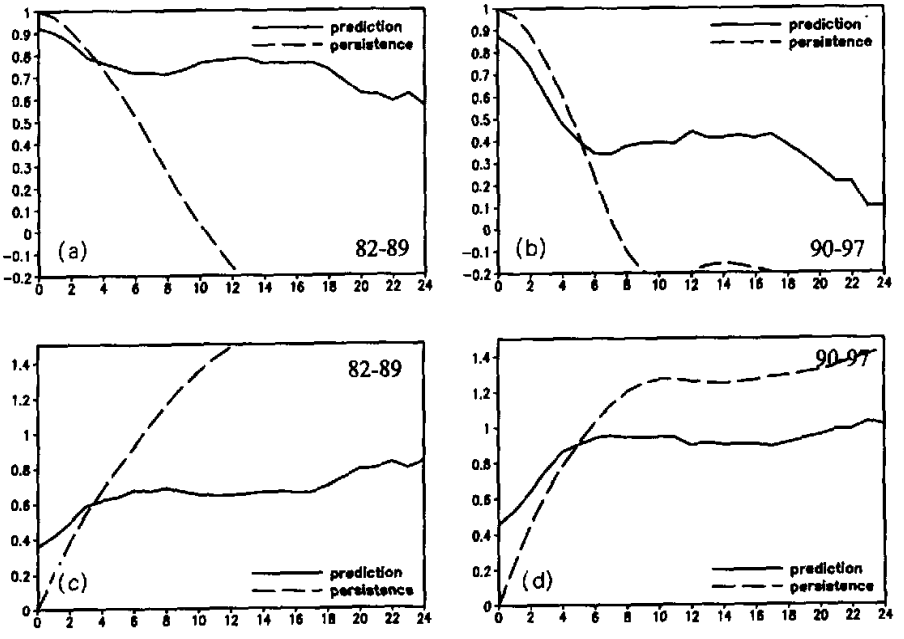

Fig. 6. Correlations (a and b) and root–mean–square errors (c and d) for the period of 1982–1989 (left panel) and 1990–1997 (right panel), respectively. Solid line: forecast; dashed line: persistence.

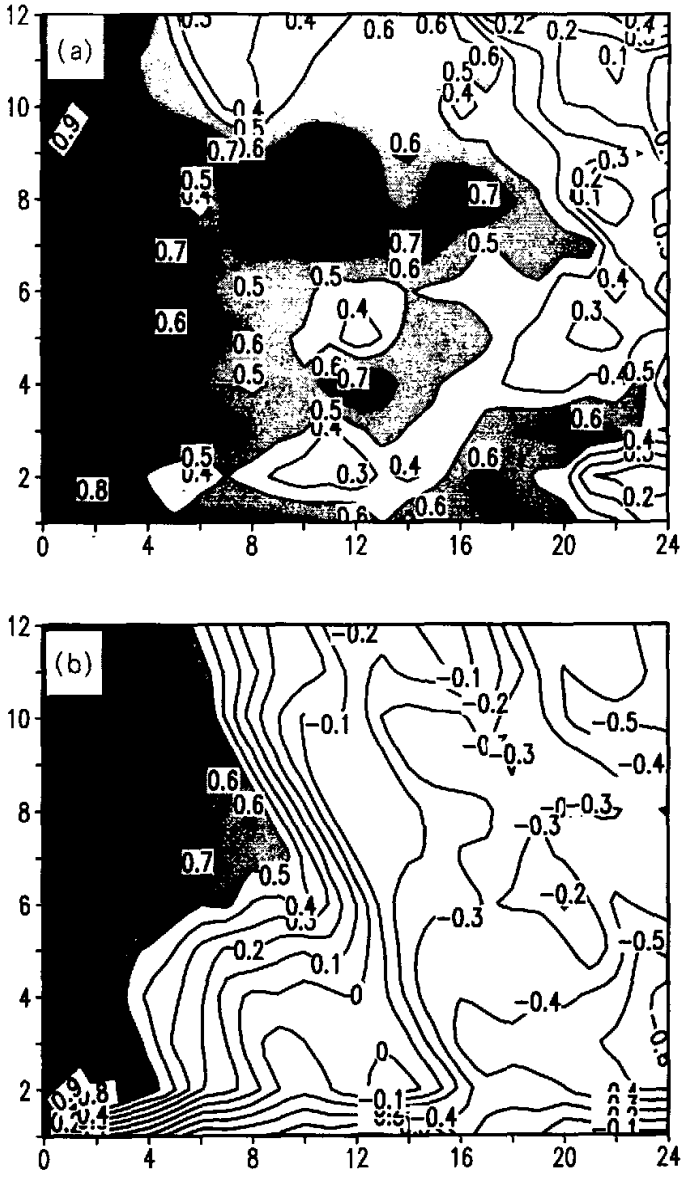

Fig. 7. The distribution of correlations with months and forecast length for forecast (a) and persistence (b). Correlations exceeding 0.5 are shaded with darker shading over 0.6.

3.2 *Time dependence*

Climate variability during the 1980s in the tropical Pacific was dominated by strong low-frequency interannual variations, while in the 1990s, especially in the first half of the

1990s, the climate state was characterized by a pattern of persistent positive SST anomalies in the tropical Pacific superimposed by several short-lived weaker warm events, e.g. in the spring 1993 and late 1994. Most of dynamical forecast systems show a higher skill in predicting the low-frequency SST variability in the 1980s and a lower skill for the short-lived variations (Ji et al., 1996). The coupled system presented here shows the similar feature of skill in predicting these SST anomalies in the tropical Pacific. Figure 6 shows the anomaly correlations and rms errors in Nino3 region for the 1980s and the 1990s, respectively. The coupled system is much more skillful in predicting the eastern equatorial Pacific SST anomalies with correlations exceeding 0.6 up to 22 months lead time, and relative smaller rms errors of about 0.7°C, in particular, the correlations of near 0.8 persist up to almost one and half years. For the variations in the 1990s, however, the correlation skill reduces rapidly to about 0.4 after 4 months in advance, and the rms errors increase to about 0.9°C for the same lead time. If the analysis samples include the predictions of 1998 and 1999, the correlations would increase to near 0.5.

To verify these forecasts further, the month-dependent skill scores are calculated. Shown in Fig. 7 is the plane of correlation distribution of SST anomalies in Nino3 region as a function of seasons and forecast length. The forecasts initiated from spring to autumn are more skillful with the correlations above 0.5 persisting to more than 15 months, while the skills exceed 0.6 up to 16 months when the predictions start from July to September. On the other hand, the skill scores of the predictions beginning from later autumn to winter are lower, which reduce rapidly to below 0.5 after 5 month forecast. It should be pointed out, in particular, that the prediction initiated from March is useful with the skills exceeding 0.6 up to 8 month length, because this is very important for the prediction of summer monsoon precipitation in China at that time.

5. Some forecast cases

A very strong El Niño occurred in 1997. The SST anomaly in the eastern equatorial Pacific turned to be negative in the summer 1998 and had been persisting until the summer 2000 (Fig. 8). Some successful near-real-time predictions of SST anomalies in the equatorial tropical Pacific had been carried out since the end of 1997. In this section, some cases of these predictions are described and compared with the observations.

The predicted SST anomaly evolution in Nino3 region from the summer 1996 to the spring 1999 is shown in Fig. 9. Three individual forecasts initiated from April, May, and June 1996 were combined into an ensemble mean. The SST anomaly would become positive in the spring 1997 and grow eventually to be a warm event in the end of 1997. Then it would decay from 1998 and turn to be negative in August 1998. The predicted phase of SST anomaly in Nino3 region is quite consistent with the observed except that the transition time in 1998 is about 3 months later than the observation. The amplitude, however, is just 1°C, too smaller than the observed 4°C. This is mainly due to the less accuracy of subsurface anomalies in thermocline, which are too weaker than the analyzed anomalies (only 20% of the analyzed ones) although they perform eastward propagation clearly, and the weak amplitude of interannual variability sustained by the coupled system as shown in Fig. 3.

The case shown in Fig. 10 starts from the spring 1998 initial states, which is also an ensemble mean of three forecasts. The SST anomaly in Nino3 region would decay gradually, but keep positive during 1998 in this forecast case that is inaccurate in comparison with the observed.

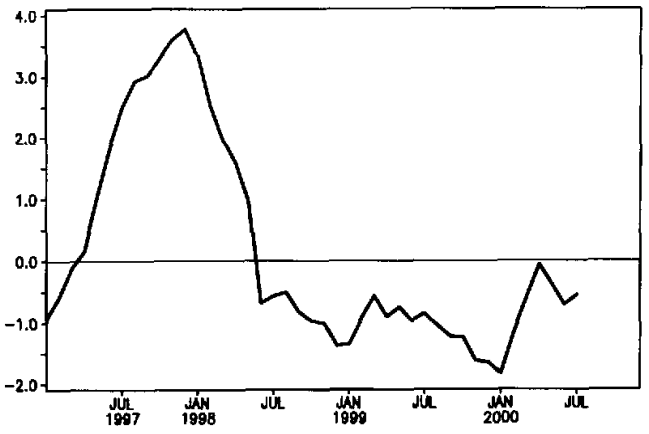

Fig. 8. Time curves of SST anomalies in Nino3 region from analysis data (Reynolds and Smith, 1994).

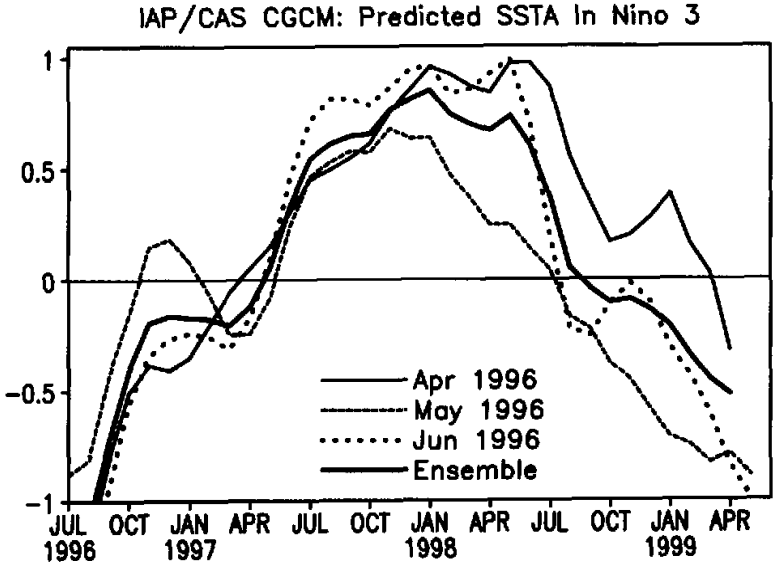

Fig. 9. Predicted SST anomaly in Nino3 region initiated from Apr. (thin solid line), May (dashed line) and Jun. (dotted line) 1996, and the ensemble of the three forecasts (thick solid line).

Figure 11 shows another case, beginning from the spring 1999, which is an ensemble of six individual predictions. The negative SST anomaly in Nino3 region would persist to the spring 2000 but the amplitude would reduce gradually according to this forecast. The

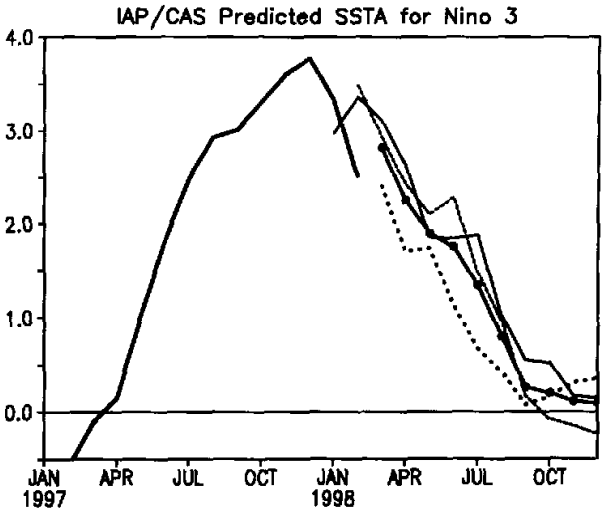

Fig. 10. Predicted SST anomaly in Nino3 region starting from Jan. (thin solid line), Feb. (dashed line) and Mar. (dotted line) 1998. The ensemble mean is presented by the solid line with dots.

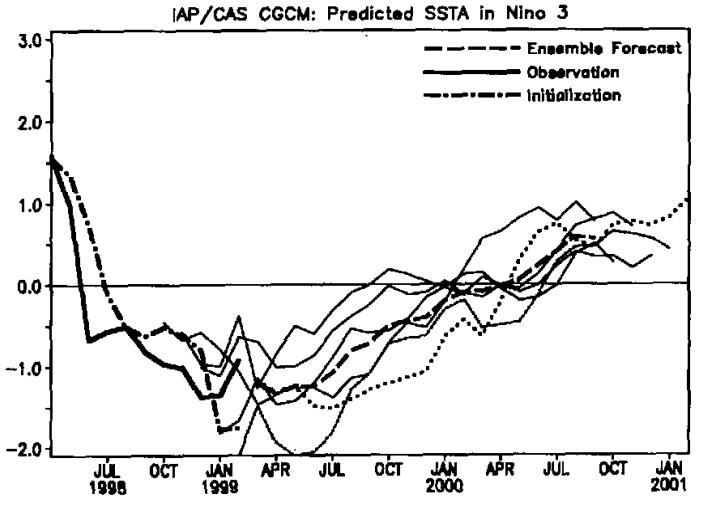

Fig. 11. Predicted SST anomaly in Nino3 region starting from Oct., Nov., Dec., 1998 and Jan., Feb., Mar., 1999, respectively. Thick dashed line: ensemble mean of six forecasts; thick solid line: observation; thick dot–and–dash line: initialization; the other lines: six individual forecasts.

observation shows that the negative anomaly indeed became weaker in the beginning of 1999, but they re–strengthened from the spring 1999 until the end of 1999 (Fig. 8). The forecast is successful in terms of persisting negative anomalies in the entire 1999 but fails in predicting the re–strengthened process.

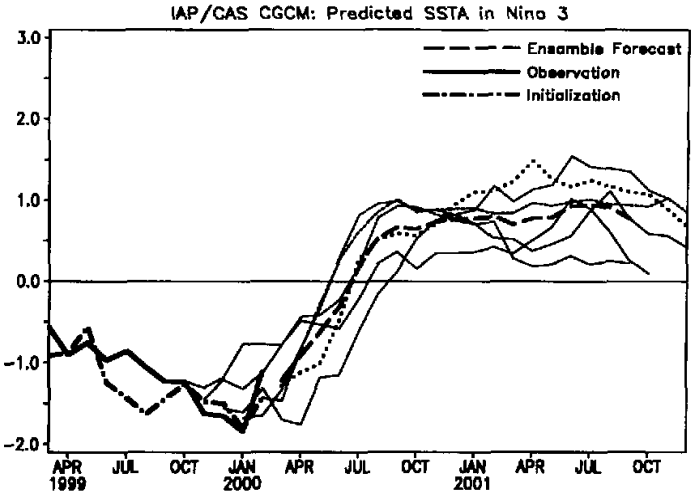

Fig. 12. Predicted SST anomaly in Nino3 region starting from Oct., Nov., Dec., 1999 and Jan., Feb., Mar., 2000, respectively. Thick dashed line: ensemble mean of six forecasts; thick solid line: observation; thick dot–and–dash line: initialization; the other lines: six individual forecasts.

In the spring 2000, a prediction combining six forecasts was also carried out (Fig. 12). The negative SST anomaly in Nino3 region would reduce and transfer to weak positive anomaly in the summer 2000. In the first half of 2001, the eastern equatorial Pacific will be in a little warm state above the normal in a sense of the forecast.

6. Summary

We described an ENSO prediction system based on the coupled atmosphere–ocean GCM developed in Institute of Atmospheric Physics, Chinese Academy of Sciences. The model's climate drift was removed by using a statistic method to correct the atmospheric variables in air–sea interface, and the climate variations in interannual scales are simulated consistent with ENSO cycle in many aspects.

An initialization scheme was designed for inducing climate anomalies by using SST anomalies in the tropical Pacific at the background of the model climatology. The numerical experiment showed that the initialization was successful in creating interannual variabilities which were needed in ENSO predictions.

The forecast system was test by performing a series of 24–month hindcast experiments, one per month for the period of November 1981 to December 1997. The system was found to produce generally good hindcasts of SST anomalies in the eastern tropical Pacific. The correlations of SST anomaly in Nino3 region exceed 0.54 up to 15 months in advance though they are lower than the persistence in the first few months. The rsm errors are less than 0.9°C for the same forecast length.

Further analyses show that the system is more skillful in predicting SST anomalies in the 1980s and less in the 1990s. This is a common discrepancy in most other dynamical forecast

systems. The model skills are also seasonal-dependent, which are lower for the predictions starting from later autumn to winter and higher for those from spring to autumn in a year-time forecast length, especially, from July to September the system performs very higher skills with anomaly correlations exceeding 0.6 up to about one and half years. It is encouraging that the prediction, beginning from March, persists 8 months long with the correlation exceeding 0.6. This is operationally useful in predictions of summer rainfall in China (Lin et al., 1999, 2000).

The results from this study are encouraging, but there are also many aspects to be improved. The initial conditions created by using the SST anomalies in the tropical Pacific are less accurate in the anomalous structure of the ocean thermocline in which the memory of the coupled system for the ENSO variability is contained. We are developing a data assimilation system similar to that of Derber and Rosati (1989), which is obviously an efficient way for inserting ocean subsurface data into the coupled system to created more accurate initial conditions that are physically in balance with the model through some appropriate modification. There are deficiencies in the present coupled model. The amplitude of the simulated interannual variability is smaller than the observation, which is presented in most coupled general circulation models. The reasons are not well known. One of the possible reasons is the coarse models' resolution, especially that the horizontal resolution in the ocean model is not higher enough in simulating the Kelvin wave well in the tropical waveguide which is regarded as the control mechanism in the ENSO evolution. Another possible reason is maybe from the coupling scheme and / or the two-component model's performance themselves, such as physical parameterization, the limited tropical region of the ocean model and so on, which suppress and / or modify the feedback between atmosphere and ocean. We are currently improving the model's simulations for both climatology and climate variation by increasing the model's resolution and modifying the coupling techniques. Another obvious deficiency is the lower skills in the 1990's predictions. Most coupled forecast systems based on dynamical frames show the similar performance. The development of ENSO in the earlier 1990s is different from that in the 1980s and this period is sometimes referred as an irregular developing period. Some researches indicted that the longer-than-interannual time scale variability (e.g. decadal variation) maybe plays an important role, which is regarded as the interaction between tropics and extratropics (Zhang et al, 1999). The coupled model applied in this forecast system is failing in simulating this long-term variation because the model's ocean is restricted in the tropical Pacific belt. In theory, therefore, the application of a global ocean model instead of the tropical one is maybe a good way to improve the forecasts, but the other difficulties caused by the global simulation could prevent the system achieving this improvement.

REFERENCES

Battisti, D. S., and A. C. Hirst, 1989: Interannual variability in a tropical atmosphere-ocean model: Influence of the basic state, ocean geometry and nonlinerity. *J. Atmos. Sci.*, **46**, 1687-1712.

Cane, M. A., S. E. Zebiak, and S. C. Dolan, 1986: Experimental forecast of ENSO. *Nature*, **321**, 827-832.

Derber, J., and A. Rosati, 1989: A global oceanic data assimilation system. *J. Phys. Oceanogr.*, **19**, 1333-1347.

Ghan, S. J., J. W. Lingaas, M. E. Shlesinger, et al., 1982: A Documentation of the OSU Two-Level Atmospheric General Circulation Model. Report No. 35, Climate Research Institute, Oregon State University, 395 pp.

Haney, R. L., 1971: Surface thermal boundary condition for ocean circulation models. *J. Phys. Oceanogr.*, **1**, 241-248

Huang, R. H., and Y. F. Wu, 1989: The influence of ENSO on the summer climate change in China and its mecha-

nism. *Advances in Atmospheric Sciences.*, **6**, 21–32.

Ji, M., A. Leetmaa, and V. Kousky, 1996: Coupled model prediction of ENSO during the 1980s and 1990s at the National Centers for Environmental Prediction. *J. Climate*, **9**, 3105–3120.

Ji, M., and A. Leetmaa, 1997: Impact of data assimilation on ocean initialization and El Niño prediction. *Mon. Wea. Rev.*, **125**, 742–753.

Kirtman, B., J. Shukla, B. Huang, Z. Zhu, and E. Schneider, 1997: Multiseasonal prediction with a coupled tropical ocean–global atmosphere system. *Mon. Wea. Rev.*, **125**, 789–808.

Latif, M., A. Sterl, E. Maier-Reimer, and M. Junge, 1993: Structure and predictability of El Niño / Southern Oscillation phenomenon in a coupled ocean–atmosphere general circulation model. *J. Climate*, **6**, 700–708.

Latif, M., and Coauthors, 1998: A review of the predictability and prediction of ENSO. *J. Geophys. Res.*, **103**, 14375–14394.

Levitus, S., 1982: Climatological Atlas of the World Ocean. NOAA Professional Paper 13, U.S. Govt. Print. Office, Washington, D. C., 173 pp.

Liang, X. Z., 1986: The design of IAP GCM and the simulation of climate and its interseasonal variability. Ph.D. Diss., Institute of Atmospheric Physics, Chinese Academy of Sciences, Beijing (in Chinese).

Lin, Z. H., X. Li, G. Q. Zhou, Y. Zhao, and Q. C. Zeng, 1999: Extraseasonal prediction of summer rainfall anomaly over China with improved IAP PSSCA. *Chinese J. Atmos. Sci.*, **23**, 351–366.

Lin, Z. H., Y. Zhao, G. Q. Zhou, and Q. C. Zeng, 2000: Prediction of summer climate anomaly over China for 1999 and its verification. *Climatic and Environmental Research*, **5**, 97–108 (in Chinese).

Pacanowski, R., and S. G. Philander, 1981: Parameterization of vertical mixing in numerical models of the tropical ocean. *J. Phys. Oceanogr.*, **11**, 1443–1451.

Reynolds, R. W., and T. M. Smith, 1994: Improved global sea surface temperature analysis. *J. Climate*, **6**, 929–948.

Schneider, E., B. Huang, Z. Zhu, et al., 1999: Ocean data assimilation, initialization, and predictions of ENSO with a coupled GCM. *Mon. Wea. Rev.*, **127**, 1187–1207.

Suarez, M. J., and P. S. Shopf, 1988: A delayed action oscillator for ENSO. *J. Atmos. Sci.*, **45**, 3283–3287.

Wang, H. J., 1997: A preliminary study on the uncertainty of shot-term climate prediction. *Climatic and Environmental Research*, **2**, 333–338 (in Chinese).

Wang, H. J., 2000: The interannual variability of east Asian monsoon and its relationship with SST in a coupled atmosphere–ocean–land climate model. *Advances in Atmospheric Sciences.*, **17**, 31–47.

Zeng, Q. C., 1983: Some numerical ocean–atmosphere coupling models. *Proceedings of the First International Symposium on the Integrated Global Ocean Monitoring*, Tallinn, USSR, Oct. 2–110.

Zeng, Q. C., X. H. Zhang, X. Z. Liang, C-G. Yuan, and S. F. Chen, 1989: *Documentation of IAP Two-Level AGCM*. TR044, DOE / ER / 60314-H1, U.S. DOE., Feb. 1989.

Zeng, Q. C., C. G. Yuan, and X. H. Zhang, et al., 1990: IAP-GCM and its application to the climate studies. *Climate Change, Dynamics and Modelling*, Beijing, China Meteorological Press, 303–330 pp.

Zeng, Q. C., C. G. Yuan, and X. Li et al., 1997: Seasonal and extra-seasonal prediction of summer monsoon precipitation by GCMs. *Advances in Atmospheric Sciences.*, **14**, 163–176.

Zhang, R. H., L. M. Rothstein, and A. J. Busalacchi, 1999: Interannual and decadal variability of the subsurface thermal structure in the Pacific Ocean: 1961–90. *Climate Dynamics*, **15**, 703–717.

Zhang, R. H., and M. Endoh, 1992: A free surface general circulation model for the tropical Pacific Ocean. *J. Geophys. Res.*, **97**, 11237–11255.

Zhang, R. H., and M. Endoh, 1994: Simulation of the 1986–1987 El Niño and 1988 La Niña events with a free surface tropical Pacific Ocean general circulation model. *J. Geophys. Res.*, **99**, 7743–7759.

Zhou, G. Q., X. Li, and Q. C. Zeng, 1999: An improved coupled ocean–atmosphere general circulation model and its numerical simulation. *Progress in Nature Science*, **9**, 374–381.

基于海气耦合环流模式的 ENSO 预测

周广庆　曾庆存

摘　要

利用一个大气大洋耦合环流模式做了 ENSO 预测研究. 通过用实测的热带太平洋区域海表温度异常叠加到耦合模式模拟的气候海温上强迫预报模式得到了预测所需的初始场, 在此基础上进行了系统性的时效为 2 年的后报试验, 时间从 1981 年 11 月至 1997 年 12 月. 对后报结果的检验表明, 在预测的前 15 个月里, Nino3 区海表温度距平总体预测相关技巧达到 0.54 以上, 均方根误差不超过 0.9°C. 预测系统对 80 年代的 ENSO 现象具有较高的预测能力, 而对 90 年代的 ENSO 事件, 其预测水平相对较低. 进一步分析表明, 预测技巧具有季节依赖性, 从秋末和冬季开始的预测相对较差而从春季到秋初开始的预测则很好. 值得一提的是从每年 3 月份开始的预测, 其 0.6 以上的相关技巧可达 8 个月, 这对中国夏季降水预测是非常重要的. 该预测系统对 1997 至 2000 年的 ENSO 现象的实际预测较为成功.

关键词: CGCM, 初始化, ENSO 预测